Available online at www.sciencedirect.com

SciVerse ScienceDirect

Ceramics International 39 (2013) 353–358

CERAMICS INTERNATIONAL

www.elsevier.com/locate/ceramint

The hydrophobicity and optical properties of the HfO_2-deposited glass

Su-Shia Lin[a,*], Chung-Sheng Liao[b]

[a]Department of Applied Materials and Optoelectronic Engineering,National Chi Nan University, Puli, Nantou Hsien 54561, Taiwan, ROC
[b]Department of Electrical Engineering, National Chi Nan University, Puli, Nantou Hsien 54561, Taiwan, ROC

Received 24 May 2012; accepted 11 June 2012
Available online 17 June 2012

Abstract

The HfO_2 thin film was deposited on the glass substrate by physical vapor deposition and exhibited good surface flatness. The coating had smaller grain size with increasing RF power. A control of lower oxidation state of Hf (Hf^{2+}) is a way to enhance the hydrophobicity of the HfO_2-deposited glass. The nonlinear refractive index of HfO_2 film on the glass substrate was measured by Moiré deflectometry, and was of the order of 10^{-8} cm^2 W^{-1}. As the RF power increased, the transparent HfO_2-deposited glass showed a blue-shift and lower transmission in the near-IR region. On comparing with the pure glass, the HfO_2-deposited glass exhibited hydrophobicity and had optical selection in the Vis–IR region for improving optical application.

Keywords: Film; Power; Hydrophobicity; Transmission

1. Introduction

During recent years, there has been a growing interest in the study of the physical properties of hafnium dioxide (HfO_2) due to its important technological applications. The properties of HfO_2 thin films depend strongly on the processing technique and conditions [1–3]. Many methods can be used to fabricate HfO_2 films, such as sol–gel [4,5], electron beam evaporation [6], ion beam assisted deposition [7], chemical vapor deposition [8], sputtering [9,10]and atomic layer deposition (ALD) [11]. HfO_2 films have been employed in optical coating because of their relatively high refractive index and good transmission in the visible range [12–14].

The glass has been widely used and has many important applications. Surfaces of a controlled hydrophobicity have many useful practical applications ranging from self-cleaning activity of window sheets to anticlouding effects in bathroom mirrors, car windows and fender mirrors. In this study, the HfO_2 thin film was deposited on glass by RF magnetron sputtering. The advantages of sputtering are in having a simple apparatus, high deposition rate, low substrate temperature, good surface flatness, and dense layer formation [15]. The major objective of this work was to investigate the influence of RF power on the HfO_2-deposited glass with respect to the hydrophobicity and optical properties.

2. Experimental procedures

The HfO_2 thin films were deposited on glass (Corning 1737) by RF magnetron sputtering. The dimension of the glass substrates was 24 mm × 24 mm × 1.1 mm. Before deposition, the substrates were ultrasonically cleaned in alcohol, rinsed in deionized water and dried in nitrogen. The target used in this study was sintered stoichiometric HfO_2 (99.95% purity, 5 cm diameter, 5 mm thickness, Target Materials Inc., USA). Sputtering was performed in an Ar atmosphere with a target-to-substrate distance of 15 cm. A turbo-molecular pump, backed by a rotary pump, was used to achieve a base pressure of 1.3×10^{-4} Pa. For the deposition of the films, the substrates were not heated. The working pressure was 1.5 Pa. An RF power (13.56 MHz, RGN-1302, ULVAC, Japan) of 60–150 W was supplied to the HfO_2 target. No external bias voltage was applied to the substrate. The rotating speed of the

*Corresponding author. Tel.: +886 49 2910960 x4771; fax: +886 49 2912238.
E-mail address: sushia@ncnu.edu.tw (S.-S. Lin).

0272-8842/$36.00
http://dx.doi.org/10.1016/j.ceramint.2012.06.033

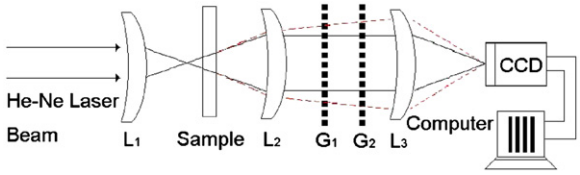

Fig. 1. Eperimental setup for measuring index of nonlinear refraction by the Moiré deflectometry technique.

substrate was 20 rpm, and the thickness of films was maintained at 100 nm.

Film thickness was measured using a surface profiler (Alpha-Step 500, TENCOR, Santa Clara, CA). Elemental compositions were investigated by X-ray photoemission spectroscopy (XPS; PHI 5000 VersaProbe, Japan). Surface morphologies and surface roughness were examined by atomic force microscopy (AFM; NS4/D3100CL/Multi-Mode, Digital Instrument, Germany). The water contact angles on samples were measured by contact angle meter (Model 100SB, Sindatek, Taiwan). Linear refractive indices of samples were recorded using a spectrometer (MP100-ST, Fremont, CA). Stress was measured by the Nano Indenter XP System (MTS Systems Corporation, MN, USA). Optical transmission spectra of samples in the visible–infrared (Vis–IR) region were obtained using a spectrophotometer (HP 8452 A diode array spectrophotometer, Hewlett Packard, Palo Alto, CA).

Moiré deflectometry is a powerful tool for measuring the nonlinear refractive indices of materials. The main advantages of the Moiré deflectometry technique are its extreme experimental simplicity, lower cost and lower sensitivity to external disturbances than other interferometric methods. In this study, this method was applied to measure the nonlinear refractive indices of HfO_2 films on glass substrates under illumination with a 5-mW He–Ne laser ($\lambda = 632.8$ nm).

Fig. 1 shows the Moiré deflectometry experimental setup that is used to measure the nonlinear refractive indices of HfO_2 films on glass substrates. Lens L_1 focused a 5-mW He–Ne laser beam (wavelength of 632.8 nm), which was re-collimated by lens L_2. The focal lengths of lenses L_1, L_2 and L_3 were all -250 mm. Two similar Ranchi gratings G_1 and G_2 with a pitch of 0.1 mm were used to construct the Moiré fringe patterns. The distance between the planes of G_1 and G_2 was set to 64 mm, which is one of the Talbot distances of the used gratings. The Talbot distances satisfy $z_t = tp^2/\lambda$ where p is the periodicity of the grating; λ is the wavelength of light, and t is an integer. In this work, the Moiré fringes were clearly formed at a Talbot distance of $z_{t=4} \approx 64$ mm. The Moiré fringe patterns were projected onto a computerized CCD camera by lens L_3, which was placed at the back of the second grating.

3. Results and discussion

The bonding conditions of hafnium on the surfaces of HfO_2 films prepared at various RF power were investigated by XPS spectra. Fig. 2 shows Hf 4 f photoelectron peaks in the XPS spectra of HfO_2 films deposited at various RF powers on glass substrates. The major peak at 17.6 eV and the shoulder peak at 18.9 eV correspond to Hf $4f_{7/2}$ and Hf $4f_{5/2}$, which are related to Hf–O bonding in the HfO_2 film deposited at 60 W. The peaks shift to lower bonding energy with RF power. The origins of the binding energy shift are suggested by a number of factors, such as charge transfer effect, presence of electric fields, environmental charge density, and hybridization [16]. Among these, charge transfer is regarded as the dominant mechanism to cause binding energy shift [16]. According to the charge transfer mechanism, removing an electron from the valence orbital generates an increase in the core electron's potential and finally leads to a chemical binding energy shift [16].

Hf $4f_{7/2}$ of the Hf^0 is at $\sim$14.0 eV in the binding energy scale [17]. Hf $4f_{7/2}$ at $\sim$16.2 eV has been suggested as the Hf $4f_{7/2}$ of the Hf^{2+} from HfO [18]. Hf $4f_{7/2}$ at $\sim$17.6 eV has been suggested as the Hf $4f_{7/2}$ of the Hf^{4+} from HfO_2 [19]. In Fig. 2, the binding energy of Hf $4f_{7/2}$ decreased from 17.6 to 16.5 eV when RF power increased from 60 to 150 W. It suggested that the contribution from lower oxidation state of Hf was probably due to Hf^{2+}. The substantial contributions from lower oxidation states have been observed at the largest oxygen deficiency [20]. According to Fig. 2, it was more favorable for HfO to form when RF power increased. It suggested that the deposited films became nonstoichiometric when RF power increased.

Table 1 shows the elemental composition of the HfO_2 films, deposited at various RF powers, obtained by XPS. The Hf content of the sputtered films increased with RF power to the HfO_2 target. The O/Hf atomic ratio decreased with RF power, suggesting that the deposited films became nonstoichiometric when RF power increased. This was in agreement with the results of Fig. 2.

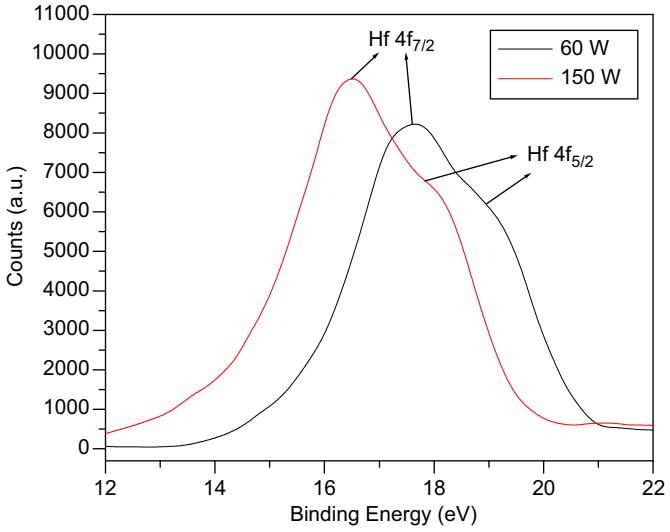

Fig. 2. Hf 4f photoelectron peaks in the XPS spectra of HfO_2 films deposited at various RF powers on glass substrates.

Table 1
Elemental composition of the HfO_2 films deposited at various RF powers on glass substrates.

RF power (W)	O content (at%)	Hf content (at%)	O/Hf
60	66.6	33.4	1.99
90	66.2	33.8	1.96
120	65.7	34.3	1.92
150	64.9	35.1	1.85

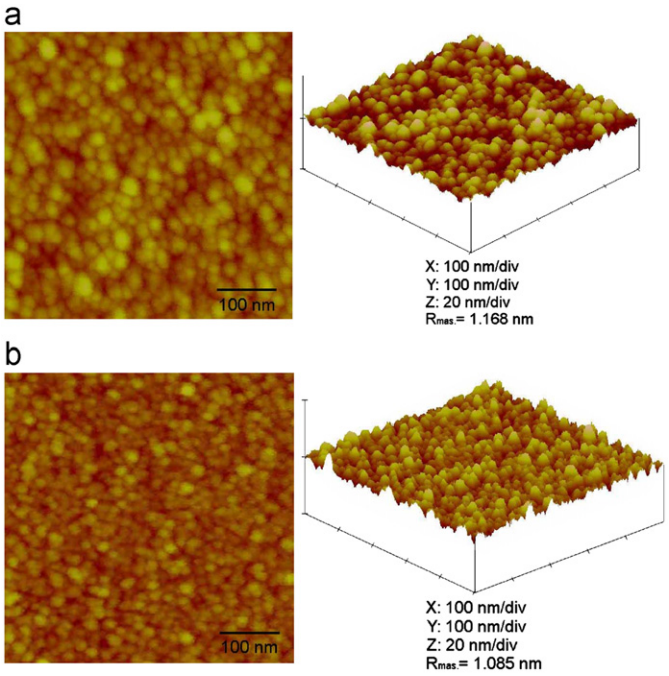

Fig. 3. The morphologies of HfO_2 films deposited at RF powers of (a) 60 W and (b) 150 W.

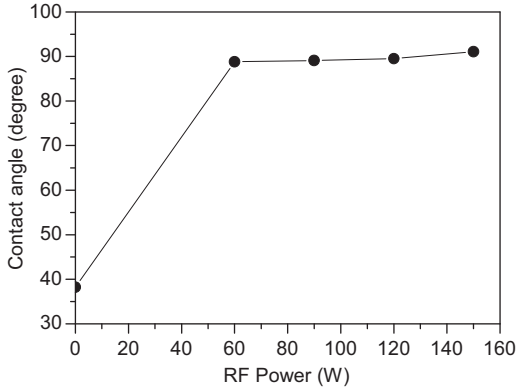

Fig. 4. Water contact angles on HfO_2 films deposited at various RF powers on glass substrates.

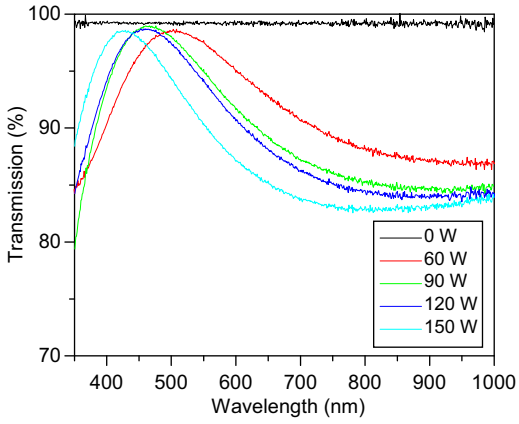

Fig. 5. The transmission in the Vis–IR region of HfO_2 films deposited at various RF powers on glass substrates.

Fig. 3 shows the morphologies of HfO_2 films deposited at RF powers of (a) 60 W and (b) 150 W. In Fig. 3a and b, HfO_2 films were composed of irregular grains with grain size of 15–35 nm and 15–20 nm, respectively. The average grain sizes decreased and became uniform with RF power. The root-mean-square (RMS) roughness decreased with RF power, but not much. The roughness values were very close to the morphologies of growing films [21].

Fig. 4 shows water contact angles on HfO_2 films deposited at various RF powers on glass substrates. The water contact angle on a pure glass substrate was 38.2°, which exhibited hydrophilic property. After depositing HfO_2 films, the water contact angles increased significantly. The water contact angle increased with the RF power and reached a maximum of 91.1° at an RF power of 150 W, and exhibited hydrophobic properties.

Wettability of a solid surface with liquids is not only governed by its chemical properties but also by its geometry [22]. By comparing Fig. 2 with Fig. 4, Hf^{2+} was more favorable to form and exhibited hydrophobic properties when RF power increased. The bonding condition of hafnium on the surface of HfO_2 film was the dominant factor in this study because the roughness had changed in a narrow range (1.085 nm–1.168 nm) with RF power. Therefore, a control of lower oxidation state of Hf (Hf^{2+}) is a way to enhance the hydrophobic properties of HfO_2-deposited glass.

Fig. 5 shows the transmission in the Vis–IR region of HfO_2 films deposited at various RF powers on glass substrates. The pure glass had no optical selection in the Vis–IR region. In the near infrared region, the transmission of HfO_2-deposited glass was lower than that of the pure glass, and decreased with RF powers. The absorption edge appeared at a short wavelength for the HfO_2 film prepared at 150 W. The shift of absorption edge may be attributed to the difference in grain size [23–25]. According to Fig. 3, the HfO_2 film prepared at 150 W contained relatively small grain size. It corresponded to the blue shift of the absorption edge. The results indicated that optical properties of HfO_2-deposited glass were significantly affected by the RF powers.

Fig. 6 shows the average visible transmission of HfO_2 films deposited at various RF powers on glass substrates. The average visible transmission was high for all samples

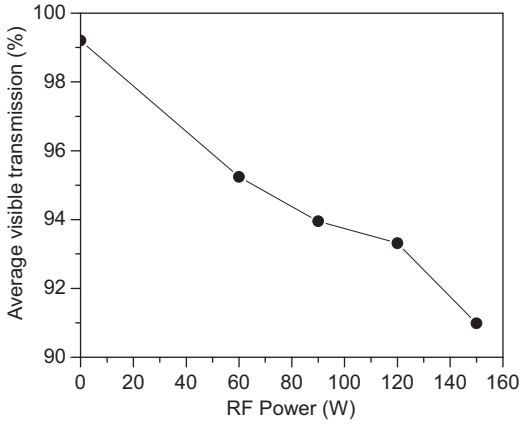

Fig. 6. The average visible transmission of HfO_2 films deposited at various RF powers on glass substrates.

($>90\%$). However, the average visible transmission decreased when RF power increased. Comparing Fig. 6 with Table 1, the HfO_2 films with lower O content had lower average visible transmission. It indicated that O content could improve the average visible transmission of HfO_2-deposited glass.

Transparent materials generally exhibit the optical Kerr effect. Nonlinear refractive indices of materials are of great interest because of potential applications in designing optical devices and laser technology [26–29]. The index of refraction, n, which depends on the radiation intensity, may be expressed in terms of the nonlinear index n_2 ($cm^2\,W^{-1}$):

$$n(r,z) = n_o + n_2 I(r,z) = n_o + \Delta n(r,z) \tag{1}$$

where n_o is the linear index of refraction, $I(r, z)$ is the irradiance of the laser beam within the sample, and $\Delta n(r, z)$ is the light-induced change in refractive index.

Based on the assumption that a Gaussian beam is traveling in the $+z$ direction, the beam irradiance can be written as

$$I(r,z) = I_0 \frac{\omega_0^2}{\omega^2(z)}\left[1-\frac{2r^2}{\omega^2(z)}\right] \tag{2}$$

where r is the radial radius of the imaginary sphere; ω_0 is the spot size of the beam at the focus; $\omega(z)=\omega_0(1+z^2/z_0^2)^{1/2}$ is the beam radius at a distance z from the position of the waist; $z_0 = \pi\omega_0^2/\lambda$ is the diffraction length of the Gaussian beam, and λ is the wavelength. The irradiance of the beam at the focus is denoted by I_0 and in terms of the input laser power, p_{in}, which equals $2p_{in}/\pi\omega_0^2$. Therefore, for a Gaussian laser beam, the radial dependence of the irradiance gives rise to a radially-dependent parabolic refractive index change near the beam axis:

$$\Delta n(r,z) = n_2 I_0 \frac{\omega_0^2}{\omega^2(z)}\left[1-\frac{2r^2}{\omega^2(z)}\right] \tag{3}$$

Moiré deflectometry is a sensitive technique for measuring changes in the refractive indices of materials. The sensitivity of this technique is determined by the minimum measurable-angle of rotation (α_{min}). The tested sample was placed at various distances from the focal point of lens L_1, and the minimum angle of rotation was obtained. The same experiment was performed by using only a pure glass substrate to check the contribution of the glass substrate to the nonlinear refraction measurement. No observed fringe rotation or change in fringe size was found.

For the thin nonlinear medium of thickness d, the lowest nonlinear refractive index can be written as

$$n_{2\,\min} = \frac{\theta f_2^2}{2z_t}\frac{f_2^2\pi\omega_0^4}{2dp_{in}z_0^2}\alpha_{\min} \tag{4}$$

and the change in the minimum refractive index is

$$\Delta n_{\min} = \frac{\theta}{z_t}\frac{f_2^2\omega_0^2}{dz_0^2}\alpha_{\min} \tag{5}$$

Fig. 7 shows the minimum nonlinear refractive indices and the change in the minimum refractive indices of HfO_2 films deposited at various RF powers on glass substrates. The nonlinear refraction index was measured to be of the order of $10^{-8}\,cm^2\,W^{-1}$ and the change in refractive index was of the order of 10^{-5}.

Fig. 8 shows the Moiré fringe patterns of (a) the pure glass and (b) the HfO_2-deposited glass. On comparing Fig. 8a with b, no rotation or change in size of the Moiré fringes was observed. It suggested that the HfO_2 film did not significantly change the number of pores for the glass.

A change of the linear refractive index caused by stress is called the photoelastic effect [30]. The linear refractive index is specified by the indicatrix, which is an ellipsoid whose coefficients are the components of the relative dielectric impermeability tensor B_{ij} at optical frequencies:

$$B_{ij}x_i x_j = 1 \tag{6}$$

The small change of the linear refractive index produced by stress is a small change in the shape, size and orientation of the indicatrix. This change is specified by the small changes in the coefficients B_{ij}.

If terms of higher-order than the first in the field of stresses are neglected, then the changes ΔB_{ij} in the

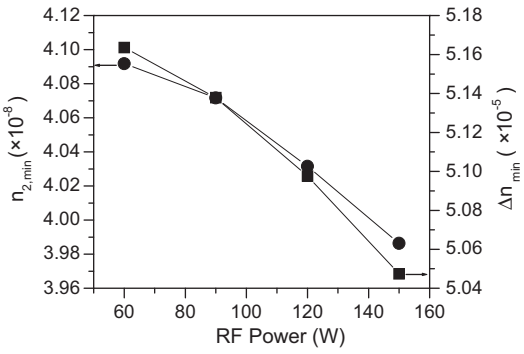

Fig. 7. The minimum nonlinear refractive indices and the change in the minimum refractive indices of HfO_2 films deposited at various RF powers on glass substrates.

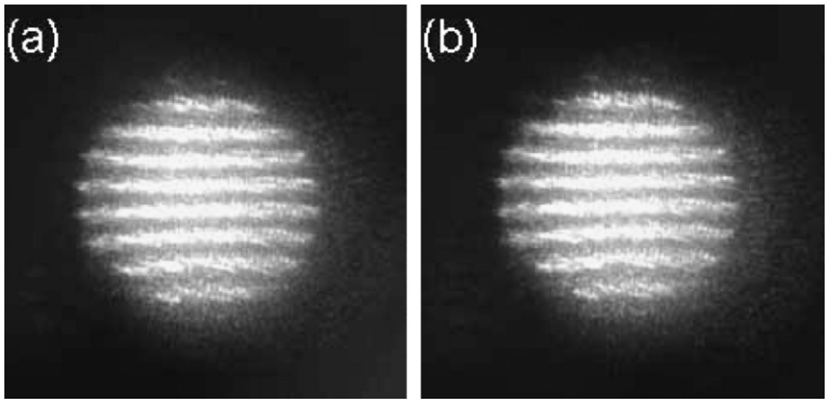

Fig. 8. The Moiré fringe patterns of (a) the pure glass and (b) the HfO_2-deposited glass.

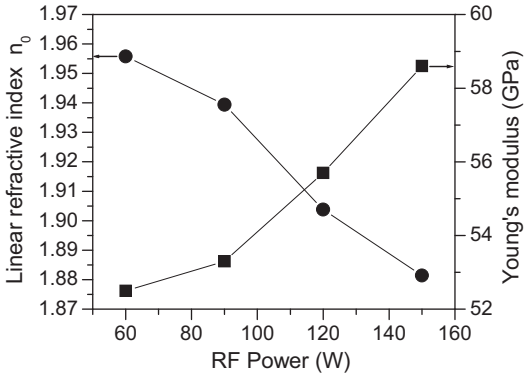

Fig. 9. The linear refractive indices and Young's moduli of HfO_2 films deposited at various RF powers on glass substrates.

coefficients are

$$\Delta B_{ij} = \varphi_{ijkl}\sigma_{kl} \text{ or } = p_{ijrs}\varepsilon_{rs} \quad (7)$$

where φ_{ijkl} and p_{ijrs} are called the piezo-optical and strain-optical coefficients, which typically have the orders of magnitude of 10^{-12} Pa^{-1} and 10^{-1} Pa^{-1}, respectively.

Based on the relation $B=1/n_0^2$, the change of linear refractive index for an isotropic film material is assumed to be [30,31]

$$\left(\frac{\partial n_0}{\partial \sigma}\right)_T = -\frac{1}{2}n_0^3\varphi \quad (8)$$

Consequently, a change in the linear refractive index due to film stress may affect the optical performance of an optical thin film, as shown in Eq. (8).

Fig. 9 shows the linear refractive indices and Young's moduli of HfO_2 films deposited at various RF powers on glass substrates. The linear refractive index decreased with RF power. However, the stress increased with RF power. The linear refractive index was found to correlate with the porosity [32,33]. It indicated that a dense HfO_2-deposited glass with a high linear refractive index and low stress could be obtained by decreasing RF power.

The value of $\Delta n/\Delta\sigma$ is reportedly similar to the stress–optical coefficient [34]. The stress–optical coefficient, $(\partial n_0/\partial\sigma)_T$, of a HfO_2-deposited glass was evaluated and was in the range from 7.72×10^{-12}–20.5×10^{-12} Pa^{-1}. Lower porosity corresponds to a lower stress–optical coefficient for the same material [33].

4. Conclusions

HfO_2 films with different properties, depending on experimental parameters, were deposited by RF magnetron sputtering on glass substrates. The lower oxidation state of Hf (Hf^{2+}) was more favorable to form and enhanced the hydrophobic properties of HfO_2-deposited glass when RF power increased. The nonlinear refraction index of the HfO_2 film on the glass substrate was measured to be of the order of 10^{-8} cm^2 W^{-1} and the change in the refractive index was of the order of 10^{-5}. As the RF power increased, the transparent HfO_2-deposited glass showed a blue-shift and lower transmission in the near-IR region. Therefore, the HfO_2-deposited glass had optical selection in the Vis–IR region for improving optical application.

Acknowledgments

The authors would like to thank the National Science Council of the Republic of China, Taiwan, for financially supporting this research under Contract no. NSC-100-2221-E-260-014.

References

[1] M. Alvisi, S. Scaglione, S. Martinelli, A. Rizzo, L. Vasanelli, Structural and optical modification in hafnium oxide thin films related to the momentum parameter transferred by ion beam assistance, Thin Solid Films 354 (1999) 19–23.
[2] P. Torchio, A. Gatto, M. Alvisi, G. Albrand, N. Kaiser, C. Amra, High-reflectivity HfO2/SiO_2 ultraviolet mirrors, Applied Optics 41 (2002) 3256–3261.
[3] D.A. Neumayer, E. Cartier, Materials characterization of Zro_2–SiO_2 and HfO_2–SiO_2 binary oxides deposited by chemical solution deposition, Journal of Applied Physics 90 (2001) 1801–1808.
[4] Z.J. Wang, T. Kumagai, H. Kokawa, J. Tsuaur, M. Ichiki, R. Maeda, Crystalline phases, microstructures and electrical

properties of hafnium oxide films deposited by sol–gel method, Journal of Crystal Growth 281 (2005) 452–457.
[5] A.R. Phani, M. Passacantando, S. Santucci, Synthesis and characterization of hafnium oxide and hafnium aluminate ultra-thin films by a sol–gel spin coating process for microelectronic applications, Journal of Non-Crystalline Solids 353 (2007) 663–669.
[6] Y. Wang, Z. Lin, X. Cheng, H. Xiao, Study of HfO_2 thin films prepared by electron beam evaporation, Applied Surface Science 228 (2004) 93–99.
[7] T. Mori, M. Fujiwara, R.R. Manory, I. Shimizu, T. Tanaka, S. Miyake, HfO_2 thin films prepared by ion beam assisted deposition, Surface and Coating Technology 169–170 (2003) 528–531.
[8] Q. Fang, J.Y. Zhang, Z. Wang, M. Modreanu, B.J. O'Sullivan, P.K. Hurley, T.L. Leedham, D. Hywel, M.A. Audier, C. Jimenez, J.P. Senateur, I.W. Boyd, Interface of ultrathin HfO_2 films deposited by UV-photo-CVD, Thin Solid Films 453-454 (2004) 203–207.
[9] X. Liu, D. Li, Influence of charged particle bombardment and sputtering parameters on the properties of HfO_2 films prepared by dc reactive magnetron sputtering, Applied Surface Science 253 (2006) 2143–2147.
[10] G. He, Q. Fang, G.H. Li, J.P. Zhang, L.D. Zhang, Structural and optical properties of nitrogen-incorporated HfO_2 gate dielectrics deposited by reactive sputtering, Applied Surface Science 253 (2007) 8483–8488.
[11] A. Deshpande, R. Inman, G. Jursich, C. Takoudis, Characterization of hafnium oxide grown on silicon by atomic layer deposition: interface structure, Micro Engineering 83 (2006) 547–552.
[12] A.J. Waldorf, J.A. Dobrowolski, B.T. Sullivan, L.M Plante, Optical coatings deposited by reactive ion plating, Applied Optics 32 (1993) 5583–5593.
[13] M. Gilo, N. Croitoru, Study of HfO_2 films prepared by ion-assisted deposition using a gridless end-hall ion source, Thin Solid Films 350 (1999) 203–208.
[14] J. Aarik, H. Mandar, M. Kirm, L. Pung, Optical characterization of HfO_2 thin films grown by atomic layer deposition, Thin Solid Films 466 (2004) 41–47.
[15] K.H. Yoon, J.W. Choi, D.H. Lee, Characteristics of ZnO thin films deposited onto Al/Si substrates by r.f. magnetron sputtering, Thin Solid Films 302 (1997) 116–121.
[16] P.S. Bagus, F. Illas, G. Pacchioni, F. Parmigiani, Mechanisms responsible for chemical shifts of core-level binding energies and their relationship to chemical bonding, Journal of Electron Spectroscopy and Related Phenomena 100 (1999) 215–236.
[17] C.D. Wagner, W.M. Riggs, L.E. Davis, J.F. Moulder, G.E. Muilenberg, Handbook of X-ray Photoelectron Spectroscopy, Perkin-Elmer Corporation,, Eden Prairie,MN, USA, 1979.
[18] S. Suzer, S. Sayan, M.M. Banaszak Holl, E. Garfunkel, Z. Hussain, N.M. Hamdan, Soft X-ray photoemission studies of Hf oxidation, Journal of Vacuum Science and Technology A 21 (2003) 106–109.
[19] O. Renault, D. Samour, D. Rouchon, P. Holliger, A.M. Papon, D. Blin, S. Marthon, Interface properties of ultra-thin HfO_2 films grown by atomic layer deposition on SiO_2/Si, Thin Solid Films 428 (2003) 190–194.
[20] S.S Lin, D.K Wu, Effect of RF deposition power on the properties of Al-doped TiO_2 thin films, Surface Coatings Technology 204 (2010) 2202–2207.
[21] G. Laukaitis, S. Lindroos, S. Tamulevičius, M. Leskelä, Stress and morphological development of CdS and ZnS thin films during the SILAR growth on (1 0 0) GaAs, Applied Surface Science 185 (2001) 134–139.
[22] A.S. Guzenda, M.G. Lipman, H. Szymanowski, J. Kowalski, P. Wojciechowski, T. Halamus, A. Tracz, Characterization of thin TiO_2 films prepared by plasma enhanced chemical vapor deposition for optical and photocatalytic applications, Thin Solid Films 517 (2009) 5409–5414.
[23] G.H. Li, L. Yang, Y.X. Jin, L.D. Zhang, Structural and optical properties of TiO_2 thin film and TiO_2+2 wt % $ZnFe_2O_4$ composite film prepared by r.f. sputtering, Thin Solid Films 368 (2000) 164–167.
[24] S.S. Lin, J.L. Huang, Effect of thickness on the structural and optical properties of ZnO films by r.f. magnetron sputtering, Surface and Coatings Technology 185 (2004) 222–227.
[25] S.S. Lin, Y.H. Hung, S.C. Chen, Optical properties of TiO_2 thin films deposited on polycarbonate by ion beam assisted evaporation, Thin Solid Films 517 (2009) 4621–4625.
[26] M.J. Soileau, W.E. Williams, N. Mansour, E.W. Van Stryland, Laser-induced damage and the role of self-focusing, Optical Engineering 28 (1989) 1133–1144.
[27] E.W. Van Stryland, Y.Y. Wu, D.J. Hagan, M.J. Soileau, K. Mansour, Optical limiting with semiconductors, Journal of the Optical Society of America B 5 (1988) 1980–1988.
[28] M.J. Soileau, W.E. Williams, E.W. Van Stryland, Optical power limiter with picosecond response time, IEEE Journal of Quantum Electronics 19 (1983) 731–735.
[29] K. Mansour, M.J. Soileau, E.W. Van Stryland, Nonlinear optical properties of carbon-black suspensions (ink), Journal of the Optical Society of America B 3 (1992) 1100–1109.
[30] J/.F. Nye, Physical Properties Of Crystals: Their Representation by Tensors And Matrices, Oxford Science, New York, 1992.
[31] W. Lukosz, P. Pliska, Determination of thickness, refractive indices, optical anisotropy of, and stresses in SiO_2 films on silicon wafers, Optics Communications 117 (1995) 1–7.
[32] G.S. Vicente, A. Morales, M.T. Gutierrez, Preparation and characterization of sol–gel TiO_2 antireflective coatings for silicon, Thin Solid Films 391 (2001) 133–137.
[33] S.S Lin, D.K. Wu, Enhanced optical properties of TiO_2 nanoceramic films by oxygen atmosphere, Journal of Nanoscience and Nanotechnology 10 (2010) 1099–1104.
[34] B. Hunsche, M. Vergöhl, H. Neuhäuser, F. Klose, B. Szyszka, T. Matthée, Effect of deposition parameters on optical and mechanical properties of MF-and DC-sputtered Nb_2O_5 films, Thin Solid Films 392 (2001) 184–190.